Korean J. Chem. Eng., 37(3), 475-481 (2020)
DOI: 10.1007/s11814-019-0472-y

pISSN: 0256-1115
eISSN: 1975-7220

Preparation and enzymatic activity of Fe_3O_4-IDA-Ni/NAD kinase magnetic catalyst

Changxia Liu†, Yadi Yang, Huafeng Gao, Xiaoshuang Bai, and Zheng-Jun Li†

College of Life Science and Technology, Beijing University of Chemical Technology, Beijing 100029, China
(*Received 19 July 2019 • accepted 25 December 2019*)

Abstract–The use of oxidoreductases as biocatalysts for industrial production of valuable compounds has a strong demand for NADP. Herein, we prepared superparamagnetic NAD kinase catalyst to synthesize NADP *in vitro*. First, Fe_3O_4 particles were synthesized through a solvothermal method, followed by the chemical modification with epichlorohydrin, iminodiacetic acid, and Ni^{2+} to yield functional Fe_3O_4 sub-microspheres. Subsequently, NAD kinase of *Escherichia coli* was overexpressed and immobilized on to the surface of magnetic sub-microspheres. The immobilized NAD kinase was used to catalyze the conversion of NAD to NADP in a cell-free system. Under optimal condition, the conversion ratio of NAD reached 91.7% and remained at 86.3% after repeated use for five times. Our study revealed that the novel magnetic NAD kinase catalyst possessed favorable properties for magnetic manipulation and NADP production.

Keywords: Fe_3O_4, Magnetic Sub-microspheres, Immobilization, NAD Kinase, NADP

INTRODUCTION

Nicotinamide adenine dinucleotides NAD/NADH and nicotinamide adenine dinucleotide phosphates NADP/NADPH are important cofactors that occur in all living cells [1]. They mainly act as electron carriers and participate in intracellular oxidation and reduction reactions [2]. The NAD/NADH pair is preferentially used for catabolic activities, whereas NADP/NADPH functions mainly in anabolic metabolisms [3]. NADP is synthesized from NAD under the catalyzation of NAD kinase (NADK). NAD kinase is a ubiquitous enzyme existing in all kinds of living organisms. The phosphorylation of NAD requires ATP or inorganic polyphosphate as phosphate donors [4]. The use of cofactor-dependent oxidoreductases as biocatalysts for industrial production of valuable compounds has a strong demand for NADP/NADPH. Nevertheless, due to the high cost and regeneration difficulty, the enzymatic production of cofactor-dependent compounds has been challenging [5]. NADP/NADPH is too expensive to be used as general agent; thus most industrial transformations requiring NADP/NADPH are conducted with whole-cell catalysts [6].

Manufacturing cost-effective NADP would be of great help to fulfill the rapidly growing needs of biotransformation. NADP has been produced by extraction from microbial cells, yet the efficiency was not satisfactory because of the low content of NADP in cells and complicated isolation procedures [7]. Therefore, enzymatic methods involving NAD kinase were developed to synthesize NADP from NAD, since the price of NAD is much lower than that of NADP. At first, the microbial cells of *Achromobacter aceris* and *Brevibacterium ammoniagenes* which had NAD kinase activity were immobilized to continuously produce NADP from NAD [7-9]. To improve enzyme stability, the thermostable NAD kinase from *Corynebacterium jlaccumfaciens* was employed for NADP production, which led to a conversion ratio of 75% and NADP concentration of 3 mM after 10 h of reaction at 50 °C [10]. Subsequently, a mass-production system was established using the purified NAD kinase from recombinant *Escherichia coli* overexpressing the *ppnK* gene of *Mycobacterium tuberculosis*, which yielded 30 mM NADP at a conversion ratio of 60% [11] (Table 1).

The native enzyme is usually hampered for industrial applications due to the instability under practical reaction conditions, difficulties in the recovery and reuse processes, and high production cost [12]. To overcome the preceding drawbacks and facilitate separation from reaction systems without losing catalytic activity, a series of enzyme immobilization techniques have been developed, including physical, covalent bonding, and affinity interactions of enzymes [13-15]. The critical factors affecting the performance of immobilized enzymes are the carriers and immobilization methods. To date, different materials have been employed for enzyme immobilization, such as organic or synthetic polymers, mesoporous materials, polysaccharides, and magnetic particles [16]. Especially, magnetic particles have recently gained special attention due to the advantage of easy separation by external magnetic treatment [17].

Iron oxide (Fe_3O_4) particles have attracted considerable attention for enzyme immobilization because of their superior characteristics including easy isolation from reaction mixtures, non-toxicity, favorable biocompatibility, large specific surface area, and chemically modifiable surfaces with different functional groups [18,19]. Naked Fe_3O_4 particles are susceptible to oxidation, acid, and alkaline conditions; thus they have been coated with mesoporous materials for practical applications [20]. The surface of Fe_3O_4 particles is usually modified with active molecules (such as epoxy, amino, thiol) to yield functional groups for covalent immobilization of enzymes [21]. A series of materials have been applied to modify the surface of Fe_3O_4 particles, including chitosan [22], polystyrene [23], silica [24], and green tea extract [25]. Further development of new approaches to improve the catalytic performance of immobilized enzymes and to reduce the cost of process is still a substantial demand.

Generally, traditional methods require controlled radical polym-

†To whom correspondence should be addressed.
E-mail: liucx@mail.buct.edu.cn, lizj@mail.buct.edu.cn

Table 1. Enzymatic synthesis of NADP by NAD kinase *in vitro*

NAD kinase source	Reaction condition	NAD convertion (%)	Reference
Brevibacterium ammoniagenes	5 mM NAD, 5 mM ATP, 37 °C, 6 h, immobilized cells with polyethylene glycoldimethacrylate	~75%	[8]
Corynebacterium flaccumfacien	4 mM NAD, 4 mM ATP, 55 °C, 10 h, permeabilized cells	75%	[10]
Mycobacterium tuberculosis	50 mM NAD, 100 mg/ml metaphosphate, 37 °C, 2 h, purified enzyme	60%	[11]
Mycobacterium tuberculosis	50 mM NAD, 100 mg/ml metaphosphate, 37 °C, 24 h, immobilized cells with polyacrylamide gel	32%	[11]
E. coli	0.9 mM NAD, 1.5 mM ATP, 55 °C, 13 h, immobilized enzyme with Fe_3O_4 particles	91.7%	This study

erizations to achieve the surface epoxidation of Fe_3O_4 particles. The coating of an epoxy polymer is a complicated reaction process that requires a series of crosslinking and initiating agents. Herein, we managed to prepare the superparamagnetic Fe_3O_4 particles through a modified solvothermal method. The chemical modification of magnetic particles was fulfilled by epichlorohydrin without polymerization processes. Then the epoxy-modified Fe_3O_4 particles were covalently connected with iminodiacetic acid (IDA), which could act as a cavity for Ni^{2+}. The metal-histidine affinity provides selective and explicit separation of target proteins expressed with hexa-histidine tag. Subsequently, NAD kinase of *E. coli* was overexpressed and immobilized on Fe_3O_4-IDA-Ni particles by metal affinity. The Fe_3O_4-IDA-Ni/NAD kinase magnetic catalyst showed favorable NAD conversion efficiency *in vitro*. Although NAD kinase of *E. coli* was demonstrated to be an ATP-NAD kinase, polyphosphate-NAD kinase exists in living organisms. A production system using polyphosphate-NAD kinase would be a promising alternative to the use of ATP-NAD kinase for the production of NADP, since inorganic polyphosphate is readily available in a much lower price than ATP.

EXPERIMENTAL

1. Chemical Reagents

Ferric chloride, ethylene glycol, sodium acetate, sodium glutamate, polyethylene glycol, 1,4-dioxane, epichlorohydrin, iminodiacetic acid (IDA), and nickel sulfate were used to prepare the Fe_3O_4-IDA-Ni particles in this study. All reagents were chemical analysis grade. The used water was distilled water.

2. Preparation of Fe_3O_4-IDA-Ni Particles

Fig. 1 shows the schematic preparation of the superparamagnetic Fe_3O_4-IDA-Ni particles to immobilize recombinant NAD

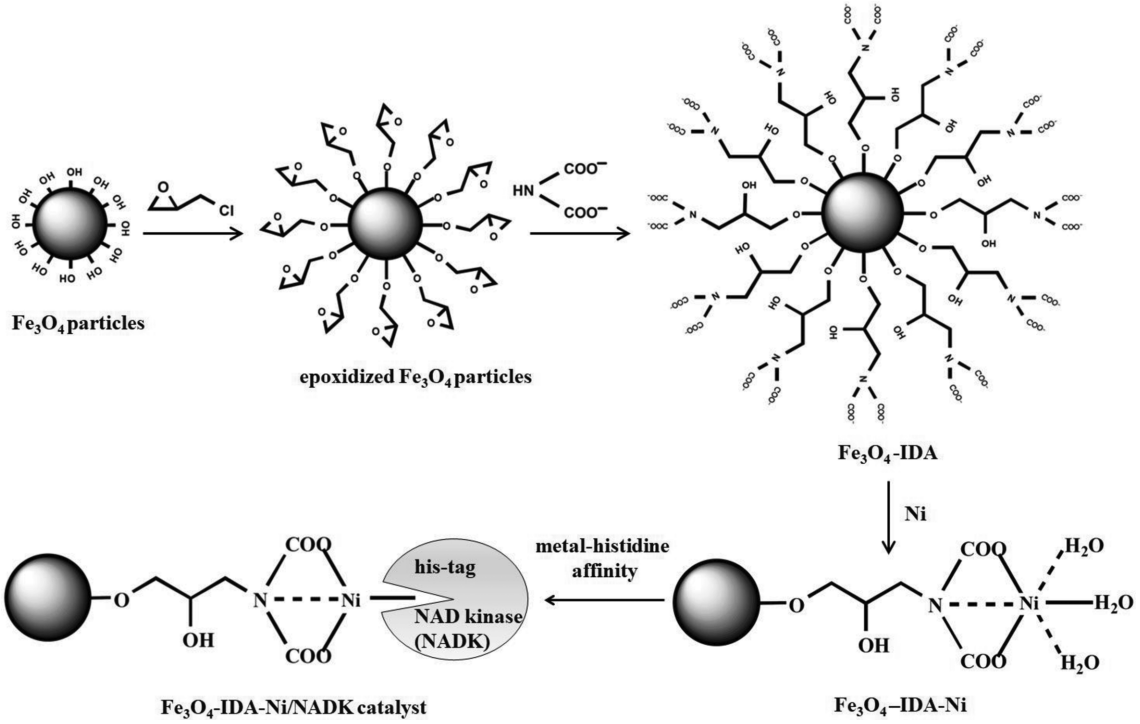

Fig. 1. Schematic illustration of the synthesis process for the preparation of NAD kinase immobilized on magnetic sub-microspheres.

kinase expressed with hexa-histidine tag. First, 1.35 g $FeCl_3 \cdot 6H_2O$ was dissolved in 40 mL ethylene glycol, followed by the addition of 2 g sodium glutamate, 1.5 g sodium acetate, and 1.5 g polyethylene glycol. The mixture was stirred vigorously and then kept at 200 °C for 8 h. The products were collected by magnetic separation, washed with deionized water and ethanol, and then dried to give Fe_3O_4 particles. Subsequently, the prepared Fe_3O_4 particles were activated by the addition of 1,4-dioxane and epichlorohydrin under alkaline condition at 25 °C and 180 rpm for 4 h. To modify the surface of magnetic particles, 0.5 g epoxidized Fe_3O_4 particles was mixed with 10 mL of 0.4 M iminodiacetic acid solution and 10 mL of 0.1 M Na_2CO_3-$NaHCO_3$ buffer (pH 9.5), and incubated at 37 °C, 250 rpm for 24 h to generate the IDA-modified Fe_3O_4 sub-microspheres, namely Fe_3O_4-IDA. Finally, the prepared Fe_3O_4-IDA (0.2 g) was added to 20 mL of 1 M $NiSO_4$ solution and incubated at 30 °C, 180 rpm for 12 h. The reaction products were washed three times with deionized water to yield Fe_3O_4-IDA-Ni particles, which was stored in 20% (v/v) ethanol solution at 4 °C for further use.

3. Characterization of the Fe_3O_4 Sub-microspheres

Transmission electron microscopy (TEM, JEM-2100F, JEOL, Japan) and field-emission scanning electron microscopy (FE-SEM, SUPRA-55, ZEISS, Germany) were used to characterize the prepared Fe_3O_4 particles. The surface groups of Fe_3O_4 particles were studied by Fourier transform infrared spectroscopy (FTIR, NEXUS-470, American Thermo-Nicolet). The magnetization curves of Fe_3O_4 particles were acquired at room temperature under a varying magnetic field using a vibrating sample magnetometer (VSM, Lake Shore 7410, USA).

4. NAD Kinase Expression

E. coli strains were cultivated in Luria-Bertani (LB) medium at 37 °C and 200 rpm. LB medium contained 10 g/L Bacto tryptone, 5 g/L yeast extract, and 10 g/L NaCl. To maintain plasmid stability, 50 μg/mL kanamycin was added to the media when required. *E. coli* JM109 was employed as the host for plasmid construction and preservation. *E. coli* BL21(DE3) was used as the host for NAD kinase expression.

The NAD kinase gene *yfjB* was amplified from the *E. coli* JM109 genomic DNA with primers yfjBF (5′-GCAGGATCCATGAATA-ATCATTTCAAGTG) and yfjBR (5′-GGGCTCGAGTGGTTTT-ATATACAGTAAAG). The PCR product was purified and digested with *Bam*HI/*Xho*I and ligated to pET28a (Novagen) cut with the same enzymes to construct plasmid pET28a-yfjB, which introduced a hexa-histidine tag to the N-terminal of NAD kinase. The overnight culture of *E. coli* BL21 (DE3) harboring pET28a-yfjB was inoculated into fresh LB broth containing kanamycin and cultivated at 37 °C and 200 rpm. When OD_{600} reached 0.6-0.8, isopropyl β-D-1-thiogalactopyranoside (IPTG) was added to a final concentration of 1 μM to induce NAD kinase expression. The cells were collected by centrifugation at 5,000 *g* for 10 min and then resuspended in 100 mM Tris-HCl buffer (pH 7.5). The cells were then subject to sonication and the supernatant was stored at 4 °C and used as the crude cell extract solution of NAD kinase.

5. NAD Kinase Immobilization

The prepared Fe_3O_4-IDA-Ni particles was mixed with 2 mL crude cell extract solution of NAD kinase, incubated at 25 °C for different time. After magnetic separation, the obtained solid particles were washed three times with Tris-NaCl buffer (pH 8.0). After washing once with 0.5 M of imidazole buffer, the obtained immobilized NAD kinase was freeze-dried and stored for further use. The amount of immobilized protein was determined by the method of Bradford with bovine serum albumin as standards.

6. NADP Production

For NAD kinase activity assay, 50 μL of crude cell extract or 0.05 g of immobilized NAD kinase was added to 1 mL of phosphate buffer (0.1 M, pH 7.4) containing 1 mM NAD, 1.5 mM ATP, and 1.5 mM $MgCl_2$. The reaction time was carried out at 50 °C for 1 min. One unit (U) of NAD kinase activity was defined as the amount of the enzyme that catalyzes the conversion of one micromole of NAD per minute under the conditions described above, and specific activity was expressed in units per milligram of total protein.

In a typical enzymatic reaction for NADP production, 0.05 g of immobilized NAD kinase was added to a 1 mL catalytic reaction mixture containing 1.5 mM ATP, 1.5 mM $MgCl_2$, and a certain amount of NAD. The reaction was carried out under different conditions. The total reaction time was 0.5, 2, 4, 8, 12, 16 h, the reaction temperature was 0, 4, 10, 20, 30, 40, 50 °C, and the substrate concentration was 0.4, 0.8, 1.2, 1.6, 2.0 mM, respectively. Once the reaction was finished, the immobilized NAD kinase was recovered by magnetic separation. The concentration of NAD and NADP was measured by high performance liquid chromatograph (HPLC) system (LC-15C, Shimadzu, Japan) equipped with a C18 column (WondaSil, 5 μm, 250×4.6 mm) and a UV detector. A mobile phase of 0.01 M KH_2PO_4 (pH 5.7) containing 10% methanol was used. The flow rate was 1.0 mL/min. The column was kept at 25 °C and the measurement was carried out at 260 nm.

The reusability of immobilized NAD kinase for NADP synthesis was studied. After enzymatic reaction, the immobilized NAD kinase was separated magnetically and washed with deionized water. Subsequently, the recovered NAD kinase was added to the fresh prepared reaction mixtures for a new round of NADP synthesis. The NAD and NADP concentrations were measured by HPLC as described previously.

RESULTS AND DISCUSSION

1. Synthesis of Fe_3O_4 Particles for Protein Purification

Fig. 1 illustrates the synthetic procedure for the preparation of Fe_3O_4-IDA-Ni/NAD kinase catalyst. First, the superparamagnetic Fe_3O_4 particles were prepared through a well-established solvothermal method [26]. Subsequently, the Fe_3O_4 particles were coated with epoxy group by epichlorohydrin. Finally, the modified Fe_3O_4 particles were connected with iminodiacetic acid (IDA) and Ni^{2+}. The cheated IDA could act as a cavity for divalent metal ion Ni^{2+}, thus providing coordination sites for the specific binding of hexa-histidine tag proteins. No polymerization reaction is required in the present synthesis process, which eliminates the use of crosslinking and initiating agents. The magnetic sub-microspheres prepared by the strategies described here were proven to be homogeneous and superparamagnetic, as described below.

2. Characterization of Fe_3O_4 Particles

The morphological features and size of the magnetic particles were observed by scanning electron microscopy (SEM, Fig. 2(a))

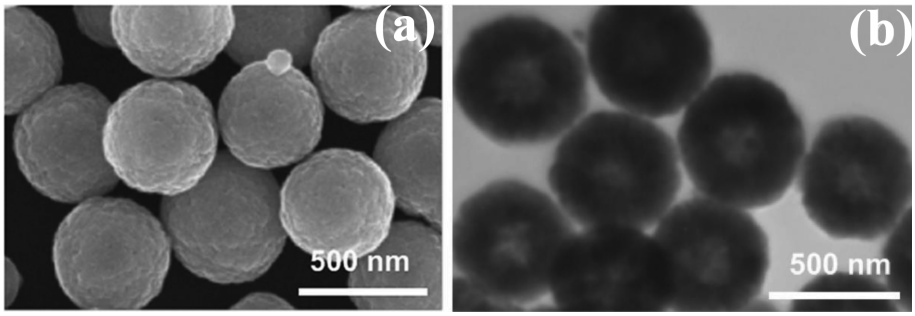

Fig. 2. SEM image (a) and TEM image (b) pattern of the prepared Fe_3O_4 particles.

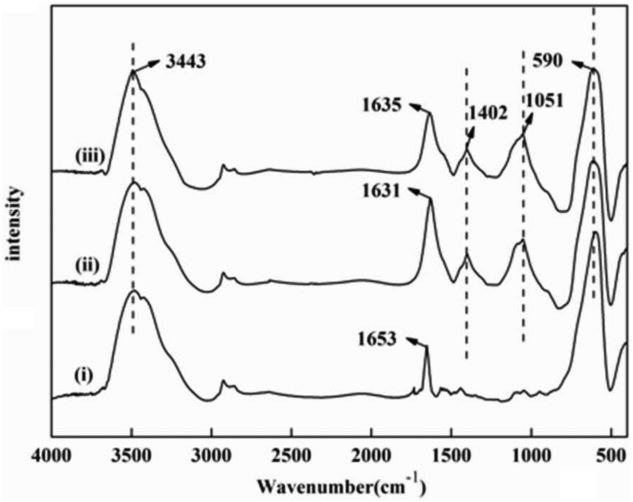

Fig. 3. FT-IR spectra of the prepared Fe_3O_4 (i), Fe_3O_4-IDA (ii), and Fe_3O_4-IDA-Ni (iii) particles.

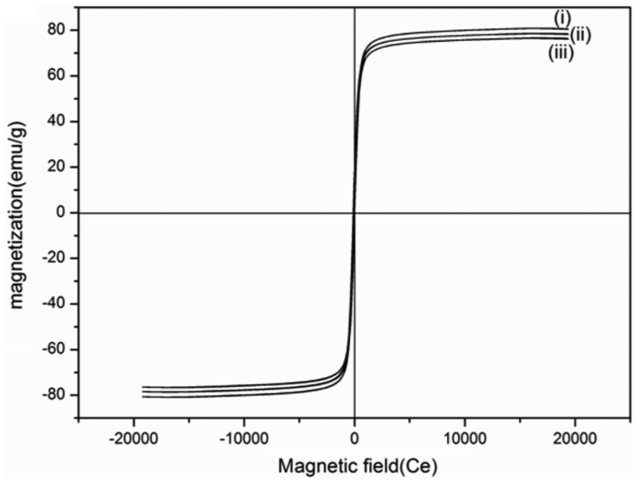

Fig. 4. Field-dependent magnetization measurement of the prepared Fe_3O_4 (i), Fe_3O_4-IDA (ii), and Fe_3O_4-IDA-Ni (iii) particles.

and transmission electron microscopy (TEM, Fig. 2(b)). As shown in Fig. 2, the naked Fe_3O_4 particles were homogeneous and monodispersed with an average diameter of approximately 400 nm. The size of Fe_3O_4 particles obtained in this study was similar to those prepared in previous reports [24].

The chemical composition of the synthesized magnetic particles was characterized by FTIR. The spectra of Fe_3O_4, Fe_3O_4-IDA, and Fe_3O_4-IDA-Ni particles are presented in Fig. 3. For the naked Fe_3O_4 particles (Fig. 3(i)), the peak at 590 cm^{-1} was ascribed to the Fe-O vibration, and peaks at 1,653 cm^{-1} and 3,443 cm^{-1} were due to the stretching vibration and bending vibration of O-H bond [27]. These results indicated that the preparation of Fe_3O_4 particles was successful. For FTIR spectra of Fe_3O_4-IDA particles (Fig. 3(ii)), the peaks at 1,051 cm^{-1} and 1,631 cm^{-1} were the signals of stretch vibrations of C-O bond and C=O, respectively [28]. In addition, the peak at 1,402 cm^{-1} was attributed to the vibration of C-N bond [29]. These results imply that the IDA was coated onto the surface of Fe_3O_4 cores. After connecting with Ni^{2+}, the stretching vibration peak of C=O bond for Fe_3O_4-IDA-Ni particles (Fig. 3(iii)) was red shifted from 1,631 cm^{-1} to 1,634 cm^{-1}, indicating the successful introduction of metal ions.

The magnetic properties of the Fe_3O_4, Fe_3O_4-IDA, and Fe_3O_4-IDA-Ni particles at room temperature were studied through measuring the magnetization curves using a vibrating sample magnetometer (Fig. 4). The saturation magnetization of the naked Fe_3O_4 particles was 80.86 emu g^{-1}. The saturation magnetization of Fe_3O_4-IDA sub-microspheres was slightly decreased to 78.63 emu g^{-1}. Furthermore, after connecting with Ni^{2+} the saturation magnetization further decreased to 76.26 emu g^{-1}, retaining 94% of the original value. There was no remanence and coercivity observed from the magnetization field curve, suggesting that prepared magnetic sub-microspheres are superparamagnetic and thus suitable for the magnetic separation of hexa-histidine tag proteins. Previously, it was reported that the saturation magnetization of the magnetic particles decreased by 30-40% after SiO_2 coating, polysaccharide coating, and lipase immobilization [24,27]. Nevertheless, only a small difference was observed between the original and modified Fe_3O_4 sub-microspheres prepared in this study, which indicated that the surface modification method presented here is superior to maintaining the magnetic properties.

3. NAD Kinase Immobilization

The prepared Fe_3O_4-IDA-Ni particles could be easily separated from the reaction system with the magnetic field. To study the application of magnetic sub-microspheres for protein purification, a total of 34 amino acids containing the hexa-histidine tag were fused to the N-terminal of NAD kinase from *E. coli*, making a fusion protein around 34 kDa. To simplify operating procedures, the crude

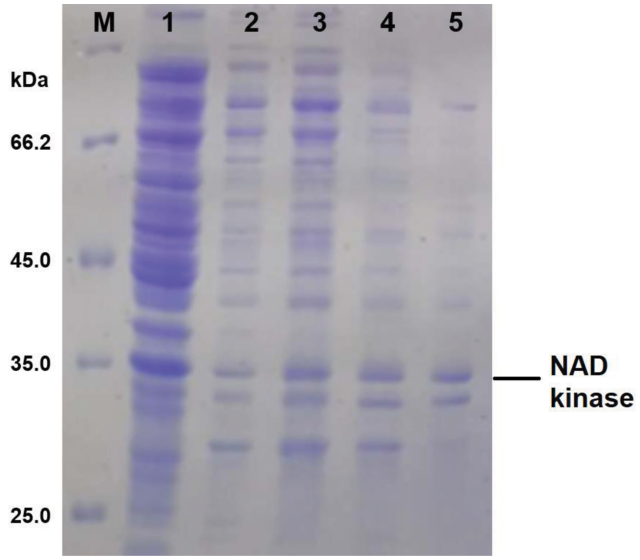

Fig. 5. SDS-PAGE analysis of recovered protein from crude cell lysate. To remove the nonspecific binding protein, imidazole solution of different concentration was applied to wash the magnetic particle. M, protein molecular weight marker (kDa); Lane 1, crude cell lysate; Lane 2, recovered protein from the crude cell lysate; Lane 3, recovered protein washed by 0.1 M imidazole; Lane 4, recovered protein washed by 0.5 M imidazole; Lane 5, recovered protein washed by 1 M imidazole.

cell lysate of *E. coli* harboring NAD kinase overexpression plasmid was directly used for immobilization with the prepared Fe_3O_4 particle. The crude cell extract solution and recovered protein samples were collected and analyzed using SDS-PAGE and Bradford assay. As shown in Fig. 5, many protein bands appeared in the SDS-PAGE gel, indicating that nonspecific binding was very significant (Lane 2). Subsequently, imidazole solution of different concentration was applied to remove the undesired proteins. The addition of 0.5 and 1 M imidazole buffer decreased the non-specific protein adsorption, yet nonspecific binding proteins were still observed (Lane 3-5). We speculate that the hexa-histidine tag NAD kinase first interacted with the Ni^{2+} of Fe_3O_4-IDA-Ni particles by metal affinity and then other protein molecules were adsorbed on the surfaces of magnetic sub-microspheres by inter-molecular interactions.

The loading efficiency, defined as ratio of the amount of protein immobilized on the magnetic spheres to that in the crude cell extract, was studied. According to the results from Bradford assay, 140 mg protein could be immobilized with 1 g Fe_3O_4-IDA-Ni particles in 5 min with a loading efficiency of 35%. In addition, results indicated that the magnetic particles were well dispersed under slight shaking after each magnetic separation.

4. NADP Production by the Fe_3O_4 Immobilized NAD Kinase

The application of immobilized NAD kinase was demonstrated by converting NAD to NADP *in vitro*. We first measured the activities of free and immobilized enzymes. The NAD kinase activity of crude cell lysate was determined to be 0.52 U/mg, where specific activity was expressed in units per milligram of total protein. By contrast, the activity of Fe_3O_4-IDA-Ni/NAD kinase magnetic catalyst was only 0.009 U/mg. The immobilization of NAD kinase on Fe_3O_4 magnetic particles significantly influenced the enzyme performance, which was probably caused by the effect of steric hindrance. It is reported that excessive enzyme loading could result in protein-protein interaction and inhibit the flexible stretching of enzyme conformation. Therefore, the enzyme may have difficulty in modulating its conformation to capture the substrate and release the product under molecular crowding condition [30,31]. Further optimization of preparing the immobilized NAD kinase should be studied to achieve better catalytic performance. For example, the introduction of a flexible spacer arm onto the supports has been applied to avoid the steric hindrance for improving enzyme activity [32].

Despite decreased specific activity, the immobilized NAD kinase exhibited desirable properties to catalyze the conversion of NAD to NADP in a cell-free system. The effects of reaction time, reaction temperature, and substrate concentration on the conversion of NAD were studied. At 25 °C and 1 mM NAD, the conversion of NAD reached the maximum of 57% at 12 h (Fig. 6(a)). Studies on behaviors of *E. coli* NAD kinase have revealed that NADPH/NADH strongly inhibited enzyme activity, while the addition of 0.1 mM NADP resulted in a 21% decrease of enzyme activity [33]. Because of the inhibition of NADP, the enzymatic reaction took as long as 12 h to reach maximal NAD conversion. At 1 mM NAD and 12 h reaction, the conversion of NAD increased with the increase of reaction temperature and the highest value of 73% was obtained at 50 °C (Fig. 6(b)). The result was consistent with previous report that *E. coli* NAD kinase was most active at 50-60 °C [33]. Nevertheless, with the increase of NAD concentration, the conversion of NAD gradually decreased (Fig. 6(c)). This was probably due mainly to the inhibition of enzyme activity by the NADP produced. Therefore, the continuous production of NADP by the immobilized NAD kinase would be helpful to achieve a high yield.

Next, response surface methodology (RSM) was applied to optimize the reaction condition. Three variables, including reaction time, reaction temperature, and NAD concentration, were employed to design the experiments. The results of the experimental design matrix and the conversion of NAD are shown in Supplementary Table 1. Subsequently, Design-Expert was applied to analyze the variance and significance test, and the results are shown in Supplementary Table 2. The significance test of the model was $p<0.05$, indicating that the model was valid and statistically significant. A correction coefficient R^2(adj) of 0.9919 can be used to simulate the real experiment. The multivariate quadratic equation obtained by response surface regression analysis is as follows:

$$Y=-1.50188+11.65458X_1+0.85263X_2-2.68438X_3+0.035833X_1X_2 +0.53125X_1X_3+0.15469X_2X_3-0.54076X_1^2-0.014856X_2^2-6.31641X_3^2$$

According to the above regression equation, the optimal reaction condition was as follows: the reaction time was 13 h, the reaction temperature was 50 °C, and the NAD concentration was 0.9 mM. The experimental conversion ratio of NAD under the optimal condition was 91.7%, close to the prediction value of 93%. As far as we know, this is the highest conversion ratio of NAD *in vitro* reported so far (Table 1).

Finally, the reusability of immobilized NAD kinase was studied. As shown in Fig. 6(d), under optimized reaction condition,

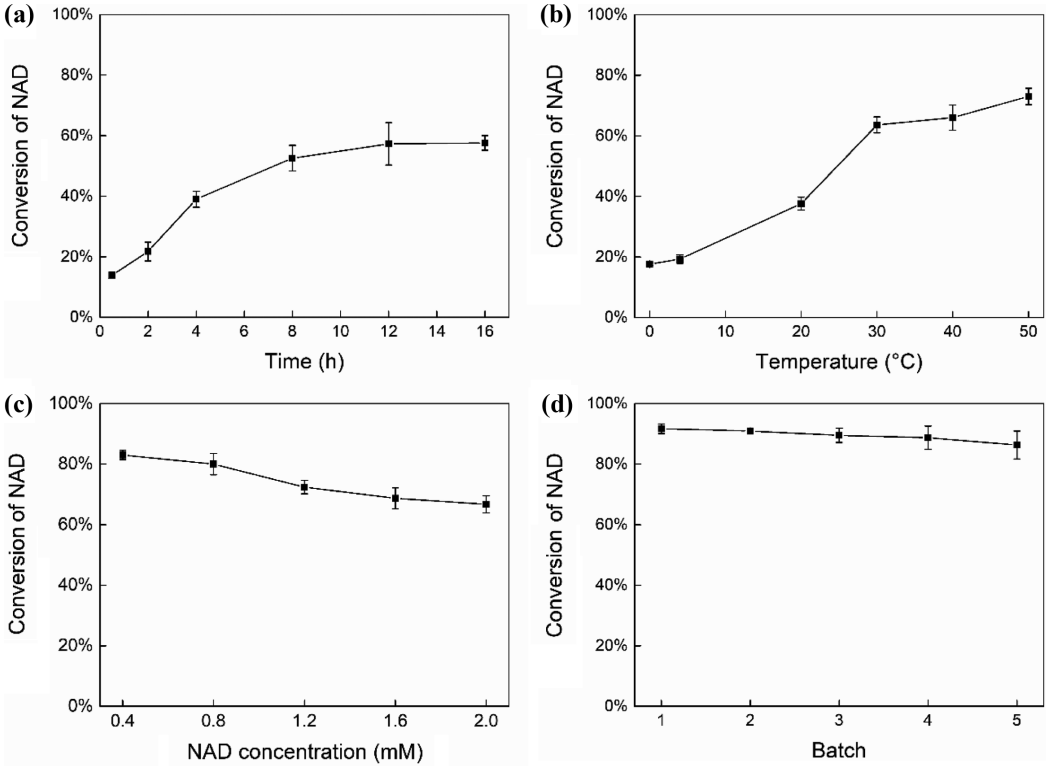

Fig. 6. Effects of reaction time (a), temperature (b), NAD concentration (c), and recycle batch (d) on the conversion of NAD.

the conversion ratio of NAD was 91.7% after the first batch of catalization. When immobilized enzyme was repeatedly used for five cycles, the conversion ratio of NAD remained at 86.3%. These data indicated that the immobilized NAD kinase has favorable stability and reusability. The application of superparamagnetic Fe_3O_4 particles for NAD kinase immobilization would be an effective strategy for economical production of NADP.

CONCLUSIONS

We have successfully presented a novel, simple and rapid procedure for the preparation of magnetic Fe_3O_4-IDA-Ni sub-microspheres with high magnetic responsiveness and functional Ni^{2+} interfaces. An amount of 140 mg protein could be immobilized with 1 g Fe_3O_4-IDA-Ni particles in 5 min. The obtained immobilized NAD kinase was used to convert NAD to NADP *in vitro*. Under optimized reaction conditions, the conversion ratio of NAD reached 91.7% and remained at 86.3% after five cycles of repeated use. The Fe_3O_4-IDA-Ni sub-microspheres shows great potential in the biotransformation applications as to effectively synthesize NADP.

ACKNOWLEDGEMENTS

This work was supported by Industry-University-Research Collaborative Innovation and Scientific and Technical Cooperation project of Xiamen Municipal Bureau of Science and Technology (3502Z20172020), Grants from National Natural Science Foundation of China (31870075), and the Fundamental Research Funds for the Central Universities (XK1802-8, PT1904). The authors declare that they have no competing financial interests.

SUPPORTING INFORMATION

Additional information as noted in the text. This information is available via the Internet at http://www.springer.com/chemistry/journal/11814.

REFERENCES

1. Y. Wang, K.-Y. San and G. N. Bennett, *Curr. Opin. Biotechnol.*, **24**, 994 (2013).
2. T. Iyanagi, *BBA-Bioenergetics*, **1860**, 233 (2019).
3. W. H. Ying, *Antioxid. Redox Sign.*, **10**, 179 (2008).
4. G. Magni, G. Orsomando and N. Raffaelli, *Mini-Rev. Med. Chem.*, **6**, 739 (2006).
5. S. Kara, J. H. Schrittwieser, F. Hollmann and M. B. Ansorge-Schumacher, *Appl. Microbiol. Biotechnol.*, **98**, 1517 (2014).
6. H. Zhao and W. A. Van Der Donk, *Curr. Opin. Biotechnol.*, **14**, 583 (2003).
7. T. Uchida, T. Watanabe, J. Kato and I. Chibata, *Biotechnol. Bioeng.*, **20**, 255 (1978).
8. Y. Tanaka, T. Hayashi, K. Kawashima, T. Yokoyama and T. Watanabe, *Biotechnol. Bioeng.*, **24**, 857 (1982).
9. K. Murata, J. Kato and I. Chibata, *Biotechnol. Bioeng.*, **21**, 887 (1979).
10. H. Matsushita, S. Yokoyama and A. Obayashi, *Can. J. Microbiol.*, **32**, 585 (1986).
11. S. Kawai, S. Mori, T. Mukai, H. Matsukawa, Y. Matuo and K. Murata, *J. Biosci. Bioeng.*, **92**, 447 (2001).

12. V. Stepankova, S. Bidmanova, T. Koudelakova, Z. Prokop, R. Chaloupkova and J. Damborsky, *ACS Catalysis*, **3**, 2823 (2013).
13. Y. Zhang, J. Zhang, X. Huang, X. Zhou, H. Wu and S. Guo, *Small*, **8**, 154 (2012).
14. X. Mu, J. Qiao, L. Qi, P. Dong and H. Ma, *ACS Appl. Mater. Inter.*, **6**, 21346 (2014).
15. R. K. Singh, M. K. Tiwari, R. Singh and J. K. Lee, *Int. J. Mol. Sci.*, **14**, 1232 (2013).
16. J. Ma, L. Zhang, Z. Liang, W. Zhang and Y. Zhang, *Anal. Chim. Acta*, **632**, 1 (2009).
17. S. Laurent, D. Forge, M. Port, A. Roch, C. Robic, L. Vander Elst and R. N. Muller, *Chem. Rev.*, **108**, 2064 (2008).
18. M. H. Liao and D. H. Chen, *Biotechnol. Lett.*, **23**, 1723 (2001).
19. N. Sohrabi, N. Rasouli and M. Torkzadeh, *Chem. Eng. J.*, **240**, 426 (2014).
20. T. Sen, A. Sebastianelli and I. J. Bruce, *J. Am. Chem. Soc.*, **128**, 7130 (2006).
21. B. Liu and J. Liu, *Nano Res.*, **10**, 1125 (2017).
22. J. Pan, Z. Ou, L. Tang and H. Shi, *Korean J. Chem. Eng.*, **36**, 729 (2019).
23. L. Jose, C. Lee, A. Hwang, J. H. Park, J. K. Song and H. J. Paik, *Eur. Polym. J.*, **112**, 524 (2019).
24. Z. Cai, Y. Wei, M. Wu, Y. Guo, Y. Xie, R. Tao, R. Li, P. Wang, A. Ma and H. Zhang, *ACS Sus. Chem. Eng.*, **7**, 6685 (2019).
25. H. Veisi, M. Ghorbani and S. Hemmati, *Mat. Sci. Eng. C*, **98**, 584 (2019).
26. Q. Zhang, Z. Zheng, C. Liu, C. Liu and T. Tan, *Colloids Surf. B.*, **140**, 446 (2016)
27. X. Guo, F. Mao, W. Wang, Y. Yang and Z. Bai, *ACS Appl. Mat. Inter.*, **7**, 14983 (2015).
28. C. Yuwei and W. Jianlong, *Chem. Eng. J.*, **168**, 286 (2011).
29. F. He, J. Fan, D. Ma, L. Zhang, C. Leung and H. L. Chan, *Carbon*, **48**, 3139 (2010).
30. Z. Lei and Q. Jiang, *J. Agric. Food Chem.*, **59**, 2592 (2011).
31. B. Hu, J. Pan, H. L. Yu, J. W. Liu and J. H. Xu, *Process Biochem.*, **44**, 1019 (2009).
32. G. Bayramoglu, B. Kaya and M. Y. Arica, *Food Chem.*, **92**, 261 (2005).
33. S. Kawai, S. Mori, T. Mukai, W. Hashimoto and K. Murata, *Eur. J. Biochem.*, **268**, 4359 (2001).

Supporting Information

Preparation and enzymatic activity of Fe_3O_4-IDA-Ni/NAD kinase magnetic catalyst

Changxia Liu†, Yadi Yang, Huafeng Gao, Xiaoshuang Bai, and Zheng-Jun Li†

College of Life Science and Technology, Beijing University of Chemical Technology, Beijing 100029, China
(*Received 19 July 2019 • accepted 25 December 2019*)

Table S1. Experimental design matrix and the corresponding conversion ratio of NAD

Std	Run	A Time (h)	B Temperature (°C)	C Concentration (mM)	Y Conversion ratio of NAD (%)
5	1	3	30	0.4	45.6(±1.6)
17	2	9	30	1.2	82.8(±1.9)
3	3	3	50	1.2	37.3(±0.4)
4	4	15	50	1.2	91.8(±2.0)
6	5	15	30	0.4	81.8(±0.8)
8	6	15	30	2.0	73.4(±0.8)
14	7	9	30	1.2	79.6(±1.3)
15	8	9	30	1.2	80.0(±1.2)
13	9	9	30	1.2	81.8(±1.0)
10	10	9	50	0.4	84.0(±0.3)
1	11	3	10	1.2	26.9(±1.7)
12	12	9	50	2.0	75.5(±0.8)
9	13	9	10	0.4	70.4(±0.6)
16	14	9	30	1.2	78.1(±1.2)
7	15	3	30	2.0	27.0(±1.0)
2	16	15	10	1.2	64.2(±1.1)
11	17	9	10	2.0	52.0(±0.3)

Table S2. ANOVA result of Design-Expert for response surface quadratic model

Source	Sum of squares	df	Mean square	F Value	p-Value Prob>F
Model	6921.21	9	769.02	219.95	<0.0001
A	3801.92	1	3801.92	1087.39	<0.0001
B	705.00	1	705.00	201.64	<0.0001
C	363.15	1	363.15	103.87	<0.0001
AB	73.96	1	73.96	21.15	0.0025
AC	26.01	1	26.01	7.44	0.0294
BC	24.50	1	24.50	7.01	0.0331
A^2	1595.72	1	1595.72	456.40	<0.0001
B^2	148.69	1	148.69	42.53	0.0003
C^2	68.81	1	68.81	19.68	0.0030
Residual	24.47	7	3.50		
Lack of fit	10.68	3	3.56	1.03	0.4679
Pure error	13.79	4	3.45		
Cor total	6945.68	16			
R-squared			0.9965		
AdjR-squared			0.9919		
C.V.%			2.81		